Super-virtual Refraction Interferometry: Field Data Example over a Colluvial Wedge

Sherif M. Hanafy, Ola AlHagan and Feras Al-Tawash, King Abdullah University of Science and Technology (KAUST), Thuwal, KSA*

SUMMARY

The theory of super-virtual refraction interferometry was recently developed to enhance the signal-to-noise ratio (SNR) of far-offset traces in refraction surveys. This enhancement of SNR is proportional to $\sqrt{N}$, and can be as high as N if an iterative procedure is used. Here N is the number of post-critical shot positions that coincides with the receiver locations. We now demonstrate the enhancement of SNR of the super-virtual refraction traces for seismic data collected over a normal fault in Saudi Arabia. Results show that both the SNR of the super-virtual data set and the number of reliable first-arrival-traveltime picks are significantly increased.

INTRODUCTION

A significant problem with current refraction surveys is that they require stronger sources in order to record first arrivals with high SNR at the far-offset traces. Without a sufficiently high SNR in the far-offset traces the refraction traveltimes cannot be accurately picked. To partly overcome this problem, Dong et al. (2006) and later Bharadwaj and Schuster (2010) developed the theory of refraction interferometry to increase the signal-to-noise ratio of head-wave arrivals. As shown in Figure 1a, the Dong et al. (2006) method correlates a pair of traces to give $\phi(\mathbf{A}, \mathbf{B})_x$, where $\mathbf{A}$ and $\mathbf{B}$ are the geophone positions and $\mathbf{x}$ is the source position. The right-hand side of Figure 1a illustrates that the resulting virtual trace will have a virtual refraction arrival with the arrival time of $\tau_{A'B} - \tau_{A'A}$. Repeating this procedure for any post-critical source position will lead to a virtual trace with the same virtual refraction traveltime, so stacking correlated traces over all post-critical source positions will yield a trace with a virtual refraction event with an enhanced SNR. This enhancement can be as high as $\sqrt{N}$, where N is the number of sources that generates this particular head wave. They demonstrated this method on land data shot over a salt dome in Utah, and later Nichols et al. (2010) demonstrated its effectiveness over a hydro geophysical research site in Idaho.

A problem with refraction interferometry is that, if only the head wave arrivals are correlated with one another, the virtual head-wave trace has the correct moveout pattern. However it has an unknown excitation time, so that, as a remedy, Dong et al. (2006) suggested that the source can be "virtually" relocated to the surface by calibrating the virtual stacked refraction trace to an observed traveltime in the raw data. Another problem is that correlation of traces typically decreases the source-receiver offset of the virtual trace because traveltimes are subtracted and are associated with shorter raypaths (Schuster, 2009). To overcome these problems, Bharadwaj and Schuster (2010) and Mallinson et al. (2011) presented an extension of refraction interferometry so that the receiver spread

could be extended to its maximum recording extent and the absolute arrival time is properly accounted for. This new method creates virtual far-offset refraction arrivals by a combination of both correlation (Figure 1a) and convolution (Figure 1b) of traces with one another to create what is denoted as super-virtual refraction traces (Figure 1c).
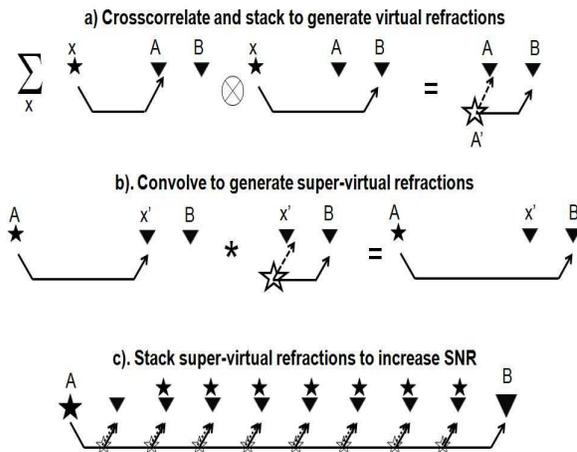

Figure 1: The steps for creating super-virtual refraction arrivals. a). Correlation of the recorded trace at $\mathbf{A}$ with that at $\mathbf{B}$ for a source at $\mathbf{x}$ to give the trace $\phi_x(\mathbf{A}, \mathbf{B}, t)$ with the virtual refraction having traveltime denoted by $\tau_{A'B} - \tau_{A'A}$. This arrival time will be the same for all post-critical source positions, so stacking $\sum_x \phi_x(\mathbf{A}, \mathbf{B}, t)$ will enhance the SNR of the virtual refraction by $\sqrt{N}$. b). Similar to that in a) except the virtual refraction traces are convolved with the actual refraction traces and stacked for different geophone positions to give the c). super-virtual trace with a SNR enhanced by $\sqrt{N}$. Here, N denotes the number of coincident source and receiver positions that are at post-critical offset.

THEORY

In this paper we follow the super-virtual interferometry method described by Bharadwaj and Schuster (2010) ,Mallinson et al. (2011), and Bharadwaj et al. (2011). They used the far-field reciprocity equation of both correlation (equation 1) and convolution (equation 2) type to create super-virtual refractions and enhance the SNR by a factor ranging between $\sqrt{N}$ and N, where N is the number of source positions associated with the generation of the head wave arrival.

Super-virtual Refraction Interferometry; Field Example

$$Im[\mathscr{G}(\mathbf{A}|\mathbf{B})^{virt\cdot}] \approx k \int_{post-crit\ sources} \mathscr{G}(\mathbf{A}|\mathbf{x})^* \mathscr{G}(\mathbf{B}|\mathbf{x})d^2x, \quad (1)$$

$$\mathscr{G}(\mathbf{B}|\mathbf{A})^{super} \approx 2ik \int_{receivers} \mathscr{G}(\mathbf{B}|\mathbf{x}')^{virt\cdot} \mathscr{G}(\mathbf{A}|\mathbf{x}')d^2x', \quad (2)$$

where the source is at $\mathbf{x}$ in Figure 1a, receivers are at $\mathbf{A}$ and $\mathbf{B}$, k is the average wavenumber, $\mathscr{G}(\mathbf{A}|\mathbf{B}) = G(\mathbf{A}|\mathbf{B})^{refract\cdot}$ represents the head wave contribution in the Green's function for a specific interface, and $\mathscr{G}(\mathbf{B}|\mathbf{A})^{super}$ denotes the super-virtual data obtained by convolving the recorded data $\mathscr{G}(\mathbf{A}|\mathbf{x}')$ with the virtual data $\mathscr{G}(\mathbf{B}|\mathbf{x}')^{virt\cdot}$ (Figure 1b).

To avoid artifacts due to a limited recording aperture and discrete sampling, Dong et al. (2006) suggested windowing about the first arrivals so that only head wave arrivals are correlated with one another.

The workflow of the super-virtual refraction interferometry is as follows:

1. Filter the raw data to remove high frequency noises.
2. Window about the first arrivals; the suggested window length is one period before the expected first arrival times and 2 to 3 periods after it.
3. Use equation 1 to generate the virtual traces.
4. Use equation 2 to generate the super-virtual traces.

One drawback of this method is, due to the limited recording aperture and a coarse spacing of the source and receivers there may be some artifacts in the super-virtual data set. In this case, either a dip filter or a least-squares approach to the redatuming might be used to mitigate such noise (Schuster and Zhou, 2006; Xue et al., 2009; Wapenaar et al., 2008).

FIELD DATA EXAMPLE

A refraction field data set is collected at the western side of Saudi Arabia along a known fault system. A total of 109 active receivers are used with receiver offsets of 3 meters, and a total of 109 shot gathers were collected with one shot located at each receiver location. The frequency spectrum of this data set shows a peak frequency of 40 Hz, so that a bandpass filter with a low cut of 5-10 Hz and a high pass of 100-120 Hz were used to remove high frequency noise (Figure 2a). In Figure 2a, far-offset traces show low SNR, and the first arrival traveltime cannot be picked.

To remedy this problem, the traces are correlated and summed (see equation 1) to create virtual traces, and then convolving these virtual traces with the raw traces yields, after stacking (see equation 2), the super-virtual traces shown in Figure 2b. It is clear that the first arrival traveltimes can be picked in the super-virtual traces compared to the raw traces in Figure 2a.

To validate the accuracy of the picked traveltimes, first arrival times were picked in the super-virtual gather and compared to

the band-pass-filtered data picks in Figure 3. The difference in these traveltimes is mostly within $T/4 = 0.006\ s$ of each other as shown in Figure 3 for shot gather 1, where T is the wavelet period. Figures 4 shows the histogram of the difference between the picked times of the band-pass-filtered and the super-virtual data sets; the histogram shows that over 90 % of the picked traces have a difference less than $T/4 = 0.006\ s$.

The super-virtual traces are obtained by the correlation and convolution of the raw traces so that the source wavelet becomes ringy. This can lead to an ambiguous identification of the first arrival, so that there is a consistent traveltime discrepancy with respect to the actual arrival time. This discrepancy can be identified by comparing the super-virtual traveltime to the actual traveltime picked from a trace with high SNR.

To demonstrate the importance of accurate first arrival picks, the tomogram of the first arrival travel-times of the bandpass filtered data set is shown in Figure 5a. The total picked traveltimes are 10,250; to eliminate unreliable picks a reciprocity test * is made so that only accurate picks are included in the inversion process, where 762 picks did not pass the reciprocity test. Here, 9,488 picks are included in the inversion, where the maximum source-receiver offset is 240m. The first arrival traveltime of the super-virtual data set is picked, and only 9,488 picks that has the same source-receiver locations as the bandpass filtered data set is inverted to generate the tomogram shown in Figure 5b. Both Figures 5a and b shows a maximum depth of penetration of 32 m and a similar velocity distribution except a low velocity anomaly is shown in Figure 5b at offsets 280 - 300 m. All first arrival traveltimes picked from the super-virtual data are then inverted (Figure 5c). Here, 842 picks did not pass the reciprocity test and 11,039 picks are inverted to generate Figure 5c. Most of the extra traveltime picks are those from far-offsets that show a low SNR in the original data set. The super-virtual tomogram shows a depth of penetration of 53 m and provide more details about the subsurface.

CONCLUSIONS

Using the super-virtual refraction interferometry method, the signal-to-noise ratio (SNR) of far-offset head wave arrivals can be theoretically increased by a factor $\sqrt{N}$; here, N is the number of receiver and source positions associated with the recording and generation of the head wave arrival. Super-virtual refraction are generated in two steps, the first is correlation of the data to generate traces with virtual head wave arrivals and the second is convolution of the data with the virtual traces to create traces with super-virtual head wave arrivals. This method is valid for any medium that generates head wave arrivals at the geophones, however, it does not enhance the SNR of the pure diving waves.

The super-virtual interferometry method is tested on a field data set. Results show that the super-virtual data set has enhances the SNR of far-offset traces so the first-arrival travel-

---

*Reciprocity test: if the difference between the first arrival traveltime picks $\tau_{S_{x1}R_{x2}}$ and $\tau_{S_{x2}R_{x1}}$ is greater than a predefined value, then both picks are rejected. Here, S_{x1} means the shot is at location $x1$, R_{x2} means the receiver is at location $x2$, S_{x2} means the shot is at location $x2$, and R_{x1} means the receiver is at location $x1$

Super-virtual Refraction Interferometry; Field Example
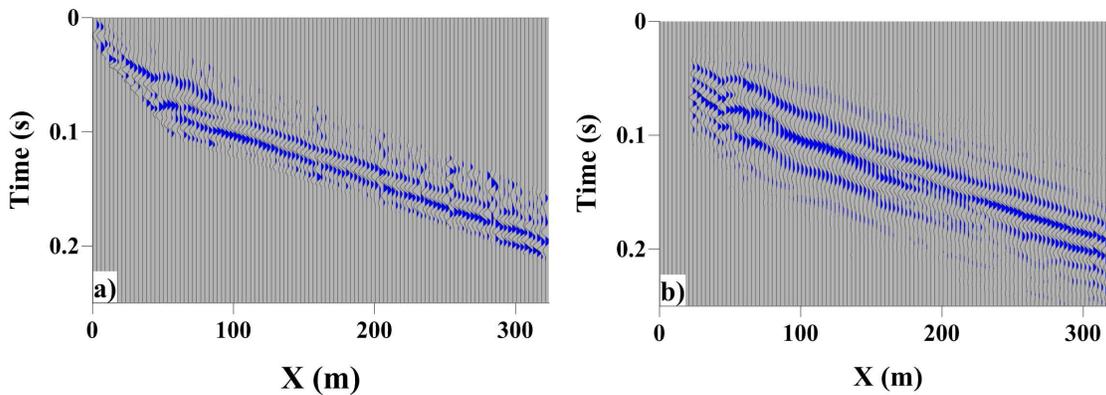

Figure 2: a) Raw shot gather after bandpass filtering and b) the super-virtual CSG with an improved SNR.
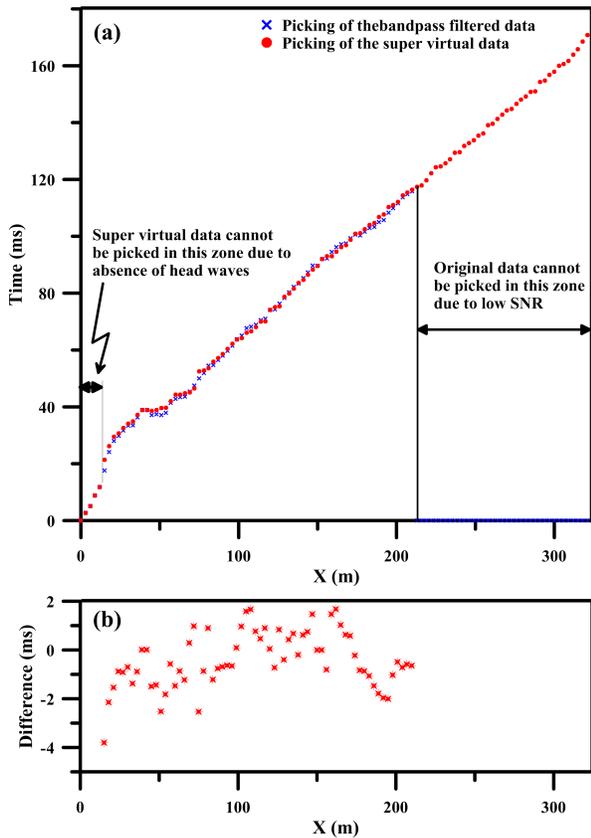

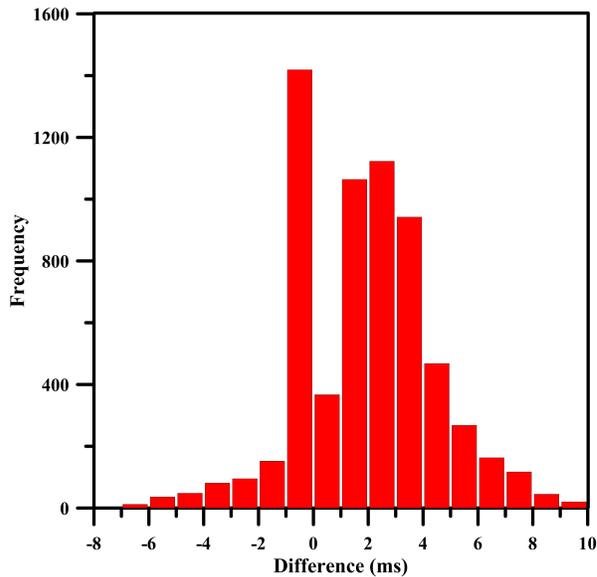Figure 3: Graph comparing both raw data and super-virtual data picks for one shot gather.

Figure 4: Plot showing the difference in travel time picks of the raw and super-virtual shot gathers of all shot gathers to estimate the error.

times of the noisy far-offset traces can be more reliably picked to extend the useful aperture of data. The first arrival travel-times of both the raw data after bandpass filter and the super-virtual data are inverted to generate a 2D velocity tomogram. Tomograms show that the depth of penetration increased from 32 to 53 meters after we included the far-offset traces, and, hence, more details about the subsurface are shown.

One drawback of this method is that, due to the limited recording aperture and a coarse spacing of the source and receivers, there will be artifacts in the super-virtual data set. In this case, a dip filter of the original data or a least-squares approach to the redatuming might be used to mitigate such noise.
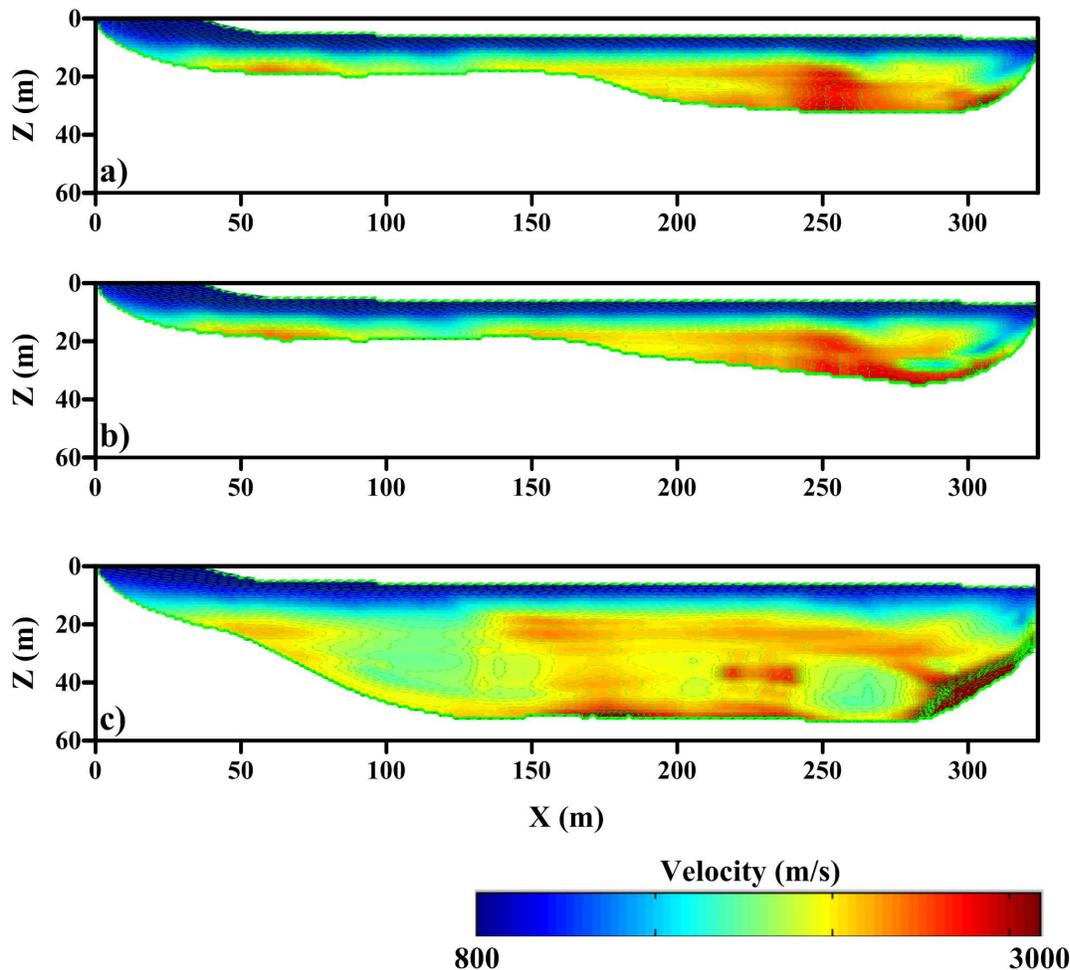

Figure 5: The velocity tomograms obtained by inverting first arrival times picked from (a) the raw data with a bandpass filter, (b) the super-virtual data set with the same locations of source-receiver pairs with high SNR, and (c) the entire super-virtual data set with high SNR.

EDITED REFERENCES

Note: This reference list is a copy-edited version of the reference list submitted by the author. Reference lists for the 2011 SEG Technical Program Expanded Abstracts have been copy edited so that references provided with the online metadata for each paper will achieve a high degree of linking to cited sources that appear on the Web.

REFERENCES

Bharadwaj, P., and G. T. Schuster, 2010, Extending the aperture and increasing the signal-to-noise ratio of refraction surveys with super-virtual interferometry: AGU Annual Meeting Abstracts.

Bharadwaj, P., G. T. Schuster, and I. Mallinson, 2011, Supervirtual refraction interferometry: Presented at the 81st Annual International Meeting, SEG.

Dong, S., J. Sheng, and G. T. Schuster, 2006, Theory and practice of refraction interferometry: 76th Annual International Meeting, SEG, Expanded Abstracts, **25**, 3021–3025.

Mallinson, I., P. Bharadwaj, G. T. Schuster, and H. Jakubowicz, 2011, Enhanced refractor imaging by super-virtual inteferometry: The Leading Edge, 30, 546–550.

Nichols, J., D. Mikesell, and K. V. Wijk, 2010, Application of the virtual refraction to near-surface characterization at the boise hydrogeophysical research site: Geophysical Prospecting, **58**, 1011–1022.

Schuster, G. T., 2009, Seismic interferometry: Cambridge University Press.

Schuster, G. T., and M. Zhou, 2006, A theoretical overview of model-based and correlation-based redatuming methods: Geophysics, **71**, no. 4, SI103–SI110, doi:10.1190/1.2208967.

Wapenaar, K., J. van der Neut, and E. Ruigrok, 2008, Passive seismic interferometry by multidimensional deconvolution: Geophysics, **73**, no. 6, A51–A56, doi:10.1190/1.2976118.

Xue, Y., S. Dong, and G. T. Schuster, 2009, Interferometric prediction and subtraction of surface waves with a nonlinear local filter: Geophysics, **74**, no. 1, SI1–SI8, doi:10.1190/1.3008543.